JCTC Journal of Chemical Theory and Computation

Article

pubs.acs.org/JCTC

Combining the Fluctuating Charge Method, Non-periodic Boundary Conditions and Meta-dynamics: Aqua Ions as Case Studies

Giordano Mancini,*[,†,‡] Giuseppe Brancato,[†,‡] and Vincenzo Barone[†,‡]

[†]Scuola Normale Superiore, Piazza dei Cavalieri 7, 56126 Pisa, Italy

[‡]Istituto Nazionale di Fisica Nucleare (INFN) Sezione di Pisa, Largo Bruno Pontecorvo 3, 56127 Pisa, Italy

ABSTRACT: We present the current status of development of our code for performing Molecular Dynamics (MD) simulations exploiting a polarizable force field based on the Fluctuating Charge (FQ) method and non-Periodic Boundary Conditions (NPBC). Continuing on the path set in a previous work, we increased the capabilities of the code by implementing a number of new features, including the following: a noniterative algorithm for rigid trigonal molecule simulations; two additional temperature coupling schemes; a meta-dynamics based approach for effective free energy evaluations. Although these are well-known algorithms, each present in one or more widely used MD packages, they have now been tested, for the first time, in the context of the FQ model coupled with NPBC. As case studies, we considered three aqueous ions of increasing charge, namely Na^+, Ca^{2+} and La^{3+}, at infinite dilution. In particular, by exploiting a computational approach recently proposed by our group and based on the metadynamics technique, we focused on the important role played by solvent polarization on ionic hydration structures, also investigating the free energy landscapes of ion coordination and the water exchange rates. Such an approach, previously tested with standard nonpolarizable models, was applied here to evaluate the effects of explicit polarization on water exchange barriers between different solvent coordination structures. Moreover, we have analyzed and discussed in some detail nonlinear electrostatic effects arising from solvent polarization while going from a mono- to a di- and trivalent ion.

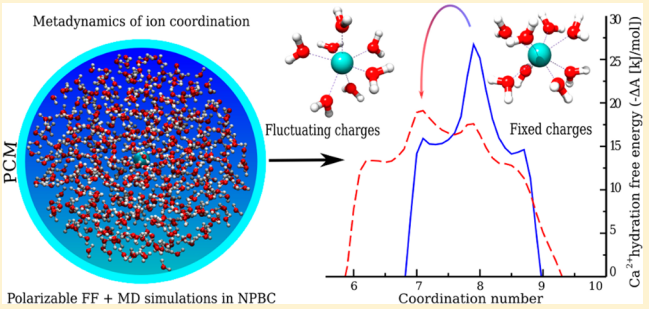

1. INTRODUCTION

For more than 30 years, scientists relied on Moore's Law to extend the scope and complexity of systems investigated with atomistic simulations, in particular by means of (classical) Molecular Dynamics[1−3] (MD). During this period a great effort has been put forth to improve the performances of MD software and its capability to describe physical systems of growing complexity with increasing accuracy, exploiting the faster hardware available at each new generation. Despite such improvements, the range of chemical phenomena amenable to classical MD is rather limited (e.g., chemical reactions, charge transfers, or radical species are generally not properly modeled); on the other hand, *ab initio* MD still suffers from severe limitations in terms of system size and extension of a statistically significant sampling, even with the latest supercomputers. Nevertheless, it is often unnecessary to include explicitly every component of very large systems (such as biological macromolecules) in full atomistic detail because in most cases the focus is on local chemical events occurring in relatively small molecular regions. Such a consideration has motivated the development of multiscale methods[4−8] developed to describe different parts of a physical system with different levels of accuracy. In this context, the introduction of explicit polarization[9] in standard force fields (FF) does provide a bridge between quantum mechanical and (nonpolarizable) classical descriptions of different subsystems. While effectively used in many practical contexts, nonpolarizable FFs disregard the effects of intra- and intermolecular polarization and may introduce severe limits, if not artifacts, when nonhomogeneous systems are considered. Especially in liquids and solutions, it has been long recognized that solvent polarization may often play a crucial role on structural, thermodynamic, and kinetic properties of chemical systems. For this reason several theoretical approaches[9] have been proposed over the years to model explicit polarization[10] within a classical framework, and in some cases, they have been integrated in widespread MD packages and FF[11−15] or have promoted the development of new packages.[16] One of the most basic examples of a nonhomogeneous solvent system, which is, at the same time, of fundamental importance for several chemical processes, is represented by the hydration of simple monatomic ions in solution,[17−19] where water molecules have, even on average, a different dipole moment going from liquid bulk to the first hydration shell of the ion.[20,21] While results obtained from MD simulations of nonpolarizable aqueous ions are generally in good agreement with experimental data[22] (especially, when ad-hoc FF are developed[23,24]), in some cases, this comparison is

Received: November 16, 2013
Published: February 11, 2014

still the object of debate, as in the case of the coordination geometry of lanthanoids.[25−28] Thus, the introduction of molecular polarization may improve these results and provide additional insights on ion microsolvation. Besides, hydration free energy changes can provide additional subtle details on the water coordination structures around ions when other data (e.g., radial distribution functions) yield comparable pictures, as discussed in the framework of the "quasi-chemical theory".[18,29]

From the computational viewpoint, in a previous study, our group has presented an implementation of a polarizable model coupled to Nonperiodic Boundary Conditions (NPBC) and showed how it could be effectively used for a wide range of applications.[30] The method chosen to treat polarization was the Fluctuating Charge[31−33] (FQ) approach, which has recently found widespread applications[11,12] for studying the properties of a variety of chemical systems in aqueous solution. We decided to adopt the FQ model for several reasons: the quantities on which it is based (electronegativity and chemical hardness) may be rigorously defined in quantum mechanical terms; it has many connections with semiempirical methods (e.g., tight-binding density functional[34,35]); and it can be easily integrated with reactive FFs, such as ReaxFF.[36] MD simulations are commonly performed using Periodic Boundary Conditions (PBC), even if a significant number of studies already pointed out the possible appearance of artifacts when dealing with long-range interactions in intrinsically nonperiodic systems, such as liquids and solutions.[37−40] Due to their complementarity with PBCs, the interest in alternative NPBC methods has been continuously increasing over the years. In addition to their conceptually easy integration with localized basis set methods, NPBC methods automatically remove artificial correlations between periodic copies of the system and, at the same time, allow to reduce the system size; this, in turn, provides increased performances as well as, in principle, faster convergence toward thermodynamic equilibrium. In a number of previous works, two of the present authors proposed and validated the GLOB[41−44] model, which couples a refined continuum model for describing the electrostatic "reaction field" of bulk solvent with an effective approach to enforce reliable nonperiodic boundary conditions that does remove spurious unphysical results due to the explicit-implicit solvent interaction at the cavity boundaries. The formal analogies existing between the FQ model and the Polarizable Continuum Model (PCM)[45] allow, in principle, the integration of FQ with GLOB, which paves the way toward a more complex, yet flexible, QM/MM multiscale approach, based on the possibility to combine different QM methods (taking advantage of the wide array of methods available in the Gaussian[46] suite of programs), classical FQ methods, and PCM for treating successive layers of a complex molecular systems, each one characterized by a decreasing level of "environmental detail" or accuracy and increasing system size.[30,47,48] Alternative approaches have been developed, wrapping up different specialized software in a higher level "meta package", as done, for example, by ChemShell,[49] taking advantage of widespread used codes and concentrating efforts especially in the communication and integration part. This latter strategy has its own advantages in terms of flexibility and fast code development. On the other hand, integrating the entire software stack may deliver enhanced performances and accuracy.

In the present paper, we have extended the capabilities of our MD code in order to thoroughly test it. In particular, we implemented a number of new features, including fixed geometries for generic trigonal molecules using a noniterative algorithm (SETTLE[50]); two additional thermostat coupling schemes, namely the Berendsen[51] thermostat and the stochastic velocity rescale method;[52] and finally, we introduced an enhanced sampling algorithm based on metadynamics.[53] As test cases, we choose three aqueous ions of increasing charge, that is, Na^+, Ca^{2+}, and La^{3+}, focusing on the effects of solvent polarization on the free energy profile of ion−water coordination and water exchange, according to a recently proposed computational approach[54] that allows to effectively estimate the free energy change of ion coordination. The role of polarization on the microsolvation of aqueous ions was analyzed by comparing results issuing from polarizable and nonpolarizable MD simulations, keeping other physical conditions as similar as possible. In particular, we have analyzed the genuine effects arising from atomic polarization and not reproducible by simple adjustments of other terms of the interaction potential, specifically the van der Waals interactions. For the sake of comparison, selected structural features (e.g., ion−water distances and coordination numbers), as issuing from nonpolarizable models, were taken as references for developing the corresponding polarizable models. Even if the accuracy of such references could be questionable, this protocol allowed us to isolate effects exclusively caused by polarization. Note that the three selected ions have been widely studied over the years[55−58] using a variety of computational and experimental approaches. For such a reason, we included available literature data, though an extended comparison with previous studies is beyond the scope of the present work.

The paper is organized as follows. A brief description of the theoretical framework is presented in section 2, along with all the computational details. In section 3.1, results on the polarizable version of the standard TIP3P[59] and SPC[60] water models are presented. Next, simulations carried out on Na^+, Ca^{2+}, and La^{3+} are reported in sections 3.2 to 3.4, and the trajectories obtained with fixed or fluctuating charges are analyzed first in terms of radial distribution functions and then using free energy landscapes, discussing how the effects pertaining only to fluctuating charges may be discerned. We also report on the effects caused by solvent polarization on water exchange rates for the three ions. In section 3.5, we include some analyses about the energetics of ion solvation using either fixed or fluctuating charges. Finally, concluding remarks and perspectives on future work are presented in section 4.

2. METHODOLOGY

2.1. Theory. In this section, we present a brief description of the FQ[30] model and of the Metadynamics method,[54] as used in this paper. The FQ method is based on the principle of electronegativity equalization (EE)[61,62] and its formulation is rooted into density functional theory. In this framework, electrons are treated as an electron gas with chemical potential, μ, whose negative value corresponds to the Mulliken's electronegativity. At equilibrium, the chemical potential will be equal in all points, that is, the electronegativity will be the same on all atoms. According to the FQ method, when an atom within a molecule moves with respect to the others or the environment, both its chemical potential and its atomic partial charge do change. In a vacuum, the electronic energy of an isolated molecule can be written as

$$E_{\text{electronic}} = \sum_{i=1}^{N} \chi_i q_i + \sum_{i=1}^{N} \eta_i q_i^2 + \sum_{i=1}^{N} \sum_{j>i} J_{ij} q_i q_j \quad (1)$$

where q_i is the atomic charge of atom i, χ its atomic electronegativity and η its hardness, which can be seen as the "stiffness" of the electron flow to or from a particular atom; the interaction kernel J_{ij} represents the interaction between pairs of nuclei and its definition depends on the actual implementation. A more formal definition of the FQ parameters χ and η (and a discussion on the definition of J_{ij}) in terms of first and second derivatives of the electronic energy with respect to the charge is presented in a previous work[30] and in the references therein. At this point, it should be noted that, in the framework of the FQ method, hardness and electronegativity can be regarded as adjustable parameters, whose values can be eventually optimized in analogy to any other force field parameter, and there are no strict requirements to get these values from either theory or experiments.[11,12] Equation 1 is easily adapted to a system composed of many molecules, and the electronegativity equalization may be conveniently reformulated in terms of a constrained minimization problem using Lagrange multipliers, where the constraints are introduced to enforce charge conservation either on the complete system or molecule-wise: both choices have positive and negative aspects and the reasons to choose either one (intramolecular charge conservation in our case) are discussed in depth in a series of papers by Rick et al.[31−33] Note that, in the framework of the FQ model, polarization is described through changes in the atomic partial charges. Besides, the total charge of each molecular moiety was constrained, so to avoid unphysical charge transfer phenomena across the whole system, as discussed in ref 30 and references therein. Accordingly, the ion charge was kept fixed during the simulations. Solving the minimization problem at each time step would be computationally cumbersome, especially for large molecular systems; however, the fluctuating charges can be dynamically propagated along with the atomic sites according to an extended Lagrangian formalism,[30,31] where the charges are endowed with a fictitious mass, which must be set to ensure adiabaticity during the simulation. In our implementation, the explicit molecular system is embedded into a spherical cavity of a polarizable continuum model (PCM). Hence, the FQs are coupled with Nonperiodic Boundary Conditions (NPBC), which are enforced using a radial potential, V_c, acting on each solvent molecule whose center of mass falls beyond a given radius, r_c, or vanishing otherwise, as expressed by a sixth-order polynomial:

$$V_c = k(r - r_c)^6 \quad (2)$$

Finite size effects are effectively taken into account surrounding this spherical box with a PCM cavity as small as possible to reduce the number of interactions concerning the explicit system, but large enough to avoid collision between the atomic fluctuating charges and the PCM apparent surface charges. In ref 30, it is also shown how the reformulation of the (electrostatic) PCM problem in a variational fashion[30] leads to a straightforward and elegant integration of the FQ and PCM formalisms. Here, we remark that the PCM response matrix does depend only on the geometry of the cavity, which, in a NVE or NVT simulation, is held fixed (currently a spherical cavity) meaning that there is basically a minimal computational overload due to the use of PCM. The boundary potential of eq 2 is not optimal and inclusion of the more refined GLOB[41,42] model in the present computational framework is currently under way. For the purpose of the present study, however, all local properties (structural, energetic, dynamical (self-diffusion)) concerning the ion hydration have been tested and provided quite reliable results.

In principle, free energy differences among distinct molecular configurations can be estimated by "standard" MD simulations, though this is often unpractical due to the extended sampling over a multidimensional configuration space usually required. For this reason, over the years, various free energy methods based on molecular simulations have been proposed and successfully applied to achieve a statistically sound sampling.[63−67] One of the most versatile techniques is represented by the so-called metadynamics,[53] already fruitfully exploited in rather different contexts. Recently,[54] we have shown how metadynamics can be effectively used to address the study of ion coordination in the liquid phase. The metadynamics methodology, as other importance sampling methods, is based on the assumption that the free energy surface of a molecular system can be properly described in terms of a few generalized or collective variables: $\Delta A = A(s)$ with s the generalized coordinate. Then, during a metadynamics run, a bias potential energy is introduced on-the-fly and undergoes cumulative and history dependent modifications based on the sampling accumulated on collective coordinates. This adaptive potential is built up to force the system to visit poorly or not yet sampled configurations and to enhance the probability to overcome barriers that are thermally out of reach. As a result, the free energy profile along a given collective variables is recovered as the opposite of such an adaptive potential; this approach not only allows a much faster sampling of the configuration space but also yields a neat and simplified picture of the free energy profile of the system under investigation. Of course, the choice of proper collective variables is of fundamental importance and must be carefully assessed in each case. In ref 54, in order to study the ion coordination in solution, we adopted the coordination number as the simplest and most chemically intuitive collective variable (s), with the prescription of defining s as given by the following continuous and smooth function:

$$s = \sum_{i=1}^{N} 1 - \frac{1}{1 + e^{-a(r_i - r_0)}} \quad (3)$$

where the index i runs over all water molecules, r_i is the distance between the ion and the i-th water molecule, r_0 is a ion−oxygen cutoff range delimiting the first hydration shell (estimated by preliminary test simulations), and a is a smoothing parameter that makes the coordination number a continuous function. The oxygen atom is considered as a proxy for the corresponding water molecule. Note that when comparing the results of metadynamics with standard MD sampling, eq 3 was used to evaluate the distribution of s from the simulated trajectory, as shown in Figures 4, 5 and 9.

2.2. Computational Details. All calculations have been performed with a local modification of the development version of the Gaussian[46] package, which includes the MD code presented in ref 30 and in this work. Overall, 21 different MD simulations have been carried out considering either pure water or an ion in aqueous solutions and comparing in each case polarizable and nonpolarizable models. Pure water simulations were carried out to test the effects of rigid geometry on the fluctuating charges while extending the integration time step. Afterward, several simulations were carried out for each ion

comparing the statistic yielded by "normal" sampling and by metadynamics. Four different sets of starting coordinates were used in all simulations: the first and second one were performed with 519 water molecules, using either the TIP3P or the SPC water model, embedded into a spherical box with a radius of 15 Å and surrounded by a PCM spherical cavity of 17 Å; the remaining considered systems were set up by adding one ion and 518 SPC (for Na^+ and Ca^{2+}) or TIP3P (for La^{3+}) water molecules in the same spherical box. The ion was located at the center of the cavity and kept frozen during the simulations. A confinement potential as described in eq 2 was applied to enforce NPBC. In all cases, the Velocity Verlet integrator was used with a time step of 0.2 (flexible bonds) or 1.0 fs (rigid bonds). An obvious improvement was thus to introduce the propagation of rigid molecules in addition to the flexible harmonic bonding potential already present in the code. Rigid bonds, not to mention other computational advantages, yield better energy conservation and are better suited for developing efficient and robust polarizable FFs. For these reasons, we implemented the SETTLE[50] algorithm originally proposed by Miyamoto and Kollmann, which allows to propagate the positions of rigid trigonal molecules using a noniterative method, which is both fast and accurate. The initially implemented Andersen thermostat,[68] which is based on a random "kick" of atoms at each time step, was not well-suited for the study of ion hydration. Thus, we implemented two additional temperature coupling methods: the stochastic velocity rescale method of Bussi, Donadio, and Parrinello[52] for its simplicity and straightforward integration in the existing code and for its ability to correctly sample a canonical phase-space distribution and the rescaling algorithm of Berendsen,[51] since it is highly tested, extremely lightweight, and useful for testing purposes. Unless otherwise specified, simulations were started at 298.15 K and temperature was kept constant by means of the stochastic velocity rescaling approach with a coupling time constant between the system and the thermostat of 10 integration time steps (i.e., either 2.0 or 10.0 fs). Charges were kept at a constant temperature of 2 K with a coupling rate equal to the integration time step. After some test simulations, the fictitious fluctuating charge mass was set to 160 au, in combination with a 0.2 fs time step, and to 180 au, with a 1.0 fs time step. All simulations were carried out for about 2 ns (pure water) or 4 ns (ion water systems) with the notable exception of La^{3+} in water, which has been simulated with fixed charges for 50 ns to allow for estimation of first shell residence time; configurations were saved every 50 (pure water) or 250 (ionic solutions) time steps; and all analyses on MD trajectories were performed discarding the first 500 ps (pure water) or 1000 ps (ionic solutions), as initial equilibration. As for metadynamics, the procedure summarized above was applied; the continuous coordination number, s, was subdivided in bins of 0.1 width; after 1000 ps of normal sampling, Gaussians were added to the bias potential energy every 100 ps; each Gaussian was 0.125 kJ/mol high and 0.1 Å wide. Although both r_0 and a of eq 3 are to be considered adjustable parameters, only r_0 was changed according to the position of the first ion hydration structure, which is more sensitive to this parameter. The a parameter was set to 4.0 $Å^{-1}$ in all cases, based on test simulations of a previous work (see ref 54). Mean residence times of water molecules in the first hydration shell were evaluated using the Impey's method.[69] This method is based on the definition of a survival probability function $P_j(t,t_n,t^*)$, where P_j is set to 1 if the j-th water molecule lies within the first hydration shell at time steps t_n and $t+t_n$, not leaving the same shell for any continuous period longer than t^*, otherwise $P_j = 0$. From P_j, it is possible to evaluate the survival function $n_{hyd}(t)$ which may be regarded as a dynamical hydration number or, better, as the time self-correlation function of the hydration shell:

$$n_{hyd}(t) = \frac{1}{N_t}\sum_{n=1}^{N_t}\sum_{j=1}^{N_{mol}} P_j(t, t_n, t^*) \quad (4)$$

where N_t is the total number of steps and the j index runs over all water molecules. At long times, $n_{hyd}(t)$ decays exponentially, with a characteristic relaxation time, τ, that defines the water MRTs in the first shell.

3. RESULTS AND DISCUSSION

3.1. Pure Water Simulations. First, we performed test simulations of rigid water models using the FQ method and analyzed, in some detail, the resulting intermolecular liquid structure with the purpose of increasing the simulation time step, δt, to typical values used with nonpolarizable force fields, that is, $\delta t = 1-2$ fs. In order to monitor the energy conservation using SETTLE in combination with NPBC, we performed long NVE simulations with the χ and η parameters taken from the original work by Rick et al.[31] and either $\delta t = 0.2$ fs with flexible bonds or $\delta t = 1.0$ fs with constrained bonds. In both cases, the energy conservation was quite satisfactory and of the same magnitude: maximum deviations were between 60 and 80 kJ/mol, that is, less than 0.4% of the potential energy of the system. Then, we switched to a NVT ensemble performing two 2 ns MD simulations with $\delta t = 1.0$ fs, rigid bonds, and either fixed or fluctuating charges; average temperature was 298.27 ± 7.01 K and 300.29 ± 15.45 K for the nonpolarizable and polarizable model, respectively; use of the simpler Berendsen thermostat for NVT simulations did not yield noticeable differences (data not shown). Next, since the following aqueous ion simulations had to be compared with nonpolarizable FFs using standard TIP3P and SPC water models, several test simulations were performed to adjust the FQ χ_{OH} parameter (η_O and η_H were not changed as in ref 30.) and the Lennard-Jones (LJ) σ and ε parameters in order to mimic the properties of the corresponding fixed charge models in terms of water dipole moment and oxygen−oxygen radial distribution function (RDF) (at least at short intermolecular distances): optimized parameters are reported in Table 1.

These water models were named TIP3P-FQ2 and SPC-FQ2 (to avoid confusion with the original parameter set presented in ref 31). In Figure 1, the O−O RDFs, $g_{OO}(r)$, as obtained from four MD trajectories based on the TIP3P model (see details in Table 1), are depicted; in particular, the plot shows the following RDFs: $\delta t = 0.2$ fs and flexible bonds, $\delta t = 0.2$ fs and rigid bonds, $\delta t = 1.0$ fs and rigid bonds (increasing the fictitious mass of charges from 160.0 to 180.0 au), and $\delta t = 1.0$ fs with a rigid geometry and fixed charges. Switching from fixed to fluctuating charges produces a widening of the $g_{OO}(r)$ first peak and an increased separation between the first and second coordination shell that resulted in a more defined $g_{OO}(r)$ second maximum; the position of the first peak is comparable with both nonpolarizable model and experimental data,[70] but trajectories obtained with FQ show a more extended structure. Such an effect is clearly visible despite the position and shape of the first peak have been optimized to better overlap with the fixed charge reference up to 3.1 Å.

Table 1. Lennard-Jones and Fluctuating Charge Parameters for the TIP3P-FQ2 and SPC-FQ2 Water Models As Used in This Work[a]

	TIP3P-FQ2	SPC-FQ2
r_{OH} (Å)	0.9572	1.0000
a_{HOH} (°)	104.52	109.47
σ_O (Å)	2.9500	3.3500
ε_O (kJ/mol)	0.7950	0.7113
χ_{OH} [kcal/(mol e)]	99.70	107.15
η_O [kcal/(mol e^2)]	371.60	367.00
η_H [kcal/(mol e^2)]	353.00	392.20

[a]The χ_{OH}, σ_O, and ε_O parameters were tuned in order to reproduce the average atomic charge and molecular dipole moment of the standard fixed charge TIP3P and SPC water models. The last row show the deviation between the average dipole moment with respect to the value of the corresponding fixed charge model. At variance with other results in the paper, χ_{OH}, η_O, and η_H parameters are measured using kcal to simplify comparison with existing literature.

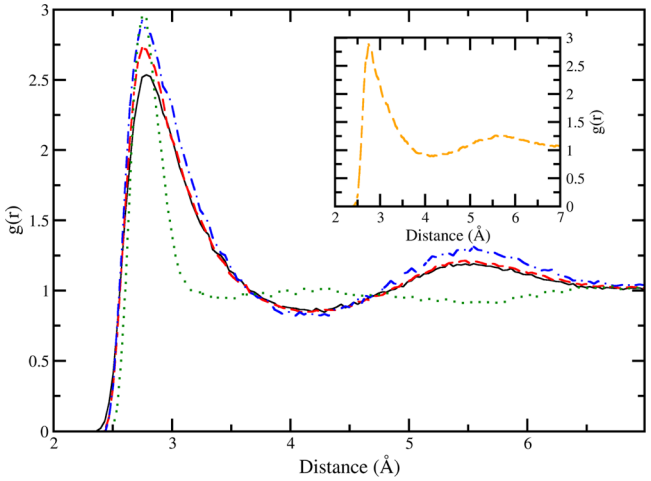

Figure 1. Results obtained for TIP3P-FQ2 using an integration step (δt) of 0.2 fs and flexible bonds (continuous black line), δt = 0.2 fs and rigid bonds (red dashed line), δt = 1.0 fs (dot-dashed blue line) and rigid bonds compared to fixed charge TIP3P with δt = 1.0 fs and a rigid geometry (green dotted line). The inset shows $g_{OO}(r)$ obtained using the SPC-FQ2 water model.

We also tried to assess the average water interaction energy using the FQ model. To this end, we compared the average potential energy (both electrostatic and Lennard-Jones contributions) sampled with the FQ simulations (δt = 1.0 fs) for both water models with those that would have been obtained applying a fixed charge parameter set on the same MD trajectory. Such an analysis was performed by considering, for each frame, the interaction energy between the nearest water molecule to the center of the sphere and all the remaining molecules within a given cutoff radius (R_C); the results obtained with increasing R_C values are summarized in Table 2. It can be observed that most of the energy differences are due to the first shell contribution (R_C = 4.0 Å) for both energy terms; it is also reasonable that the LJ energy difference decreases as more water molecules are included since σ_{FQ} and ε_{FQ} were tuned to compensate structural differences in the first shell.

Finally, Figure 2 shows the molecular dipole moment distributions obtained using fluctuating charges, compared with the corresponding reference dipole moments (2.35 D for

Table 2. Average Differences between the Actual Potential Energies (Electrostatic and Lennard-Jones) Calculated Along the FQ Trajectories (δt = 1.0 fs) and Those That Would Have Been Obtained with a Fixed Charge Model on the Same Coordinates (see Table 1), Obtained Using Increasing Cut-off Radii (R_C)

	SPC-FQ2		TIP3P-FQ2	
	ΔE_{Elec} (kJ/mol)	ΔE_{LJ} (kJ/mol)	ΔE_{Elec} (kJ/mol)	ΔE_{LJ} (kJ/mol)
R_C = 4.0 Å	1.85	20.92	3.49	3.69
R_C = 7.0 Å	1.98	19.90	3.79	3.35
R_C = 10.0 Å	1.98	19.70	3.92	3.29
R_C = 13.0 Å	2.03	19.65	3.97	3.27

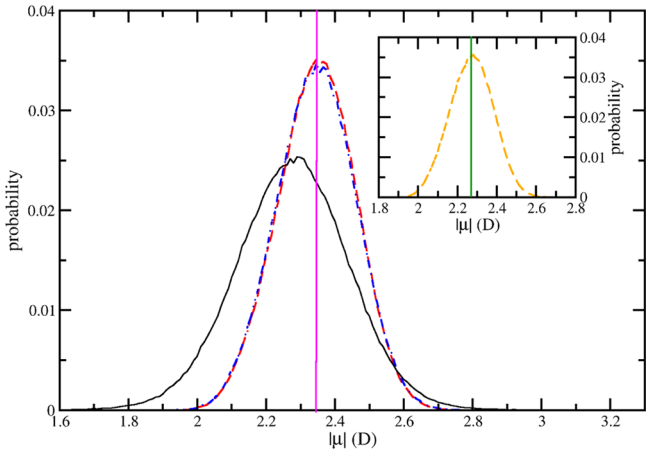

Figure 2. Dipole moment distributions for the TIP3P-FQ2 and SPC-FQ2 water models (inset). For the TIP3P-FQ2 model the distributions were obtained using an integration step of 0.2 fs and flexible bonds (continuous black line), 0.2 fs and rigid bonds (red dashed line), 1.0 fs (dot-dashed blue line). The dipole moment value for a fixed charge TIP3P water molecule with fixed charges is 2.35 D (purple vertical line). For the SPC-FQ2, see inset on the right, model the distribution (orange dashed line) was obtained using a fixed geometry and a time step of 1.0 fs; the dipole moment value for a fixed charge SPC water molecule is 2.27 D (green vertical line).

TIP3P[71] and 2.27 D for SPC[72]). When using δt = 1.0 fs and SETTLE, a Gaussian distribution centered on the reference value is obtained with both TIP3P-FQ2 and SPC-FQ2 models. Furthermore, the use of flexible bonds shifts the average water dipole moment to smaller values due to the increase of the average HOH angle (107°) with respect to standard TIP3P (104.51°). Summarizing, integrating SETTLE and NVT simulations in the FQ/PCM framework allows to extend the capabilities of the code to the nanosecond time scale without loss of theoretical accuracy; besides, even if it is well-known that such simplified water models imperfectly describe bulk liquid properties and some improvements might be expected by the inclusion of out-of-plane polarizable sites, we think that, nevertheless, they suit the aim of this work about evidencing polarization effects on ion−water systems, as compared to standard nonpolarizable force fields.

3.2. Na^+ in Water. *3.2.1. Radial Distribution Functions.* The first ion−water system studied was Na^+. The effects of fluctuating charges on the structure and dynamics of the first hydration shell of Na^+ have been studied by performing two simulations with either SPC or SPC-FQ2; in both cases, the standard GROMOS96[73] LJ potential was employed to model

dx.doi.org/10.1021/ct400988e | J. Chem. Theory Comput. 2014, 10, 1150−1163

Table 3. Lennard-Jones Parameters Used with Fixed and Fluctuating Charge Simulations for the Three Ion−Water Systems Studied[a]

LJ	Na1	Na2	Na3	Na4	Ca^{2+} fix.	Ca^{2+} FQ	La^{3+} fix.	La^{3+} FQ
σ (Å)	2.8900	2.8900	2.5000	1.7500	3.1600	2.8000	3.7500	3.1500
ε (kJ/mol)	0.0628	0.0628	0.0628	10.460	0.5060	0.5060	0.2150	0.3350

[a]Note that the force field definitions and combination rules are different between GROMOS (used for Na^+ and Ca^{2+} in combination with SPC or SPC-FQ2) and OPLS (used for La^{3+} in combination with TIP3P or TIP3P-FQ2). The four simulation performed for Na^+ have labeled **Na1** (fixed charges), **Na2** (FQ), **Na3** (FQ), **Na4** (FQ). For Ca^{2+} and La^{3+} trajectories with fixed and fluctuating charges have been indicated with either "fix." or FQ.

the Na^+−O interaction. Then, two additional simulations with polarizable water have been carried out in which the same LJ potential has been slightly modified. As stated in the Introduction, such modifications of nonbonded interactions were considered in order to resemble as much as possible the structural properties of the corresponding nonpolarizable counterpart, so to better focus on those effects specifically caused by solvent polarization. To be specific, initially, only the ion−oxygen distance (i.e., the position of the $g(r)$ first peak; IOD hereafter) was reproduced by modifying the LJ $\sigma(Na^+-O)$ parameter. Afterward, also the first peak width and height were rather well reproduced by modifying both $\sigma(Na^+-O)$ and $\varepsilon(Na^+-O)$. Several test simulations were performed in both cases, evaluating the Na^+−O RDF after 500 ps to accept or reject the modified parameters and finally two additional production runs with these modified potentials were performed. For the sake of convenience, in the following we will label Na^+ simulations as follows: **Na1** for standard nonpolarizable GROMOS96, **Na2** for GROMOS96 LJ potential and FQs, **Na3** for modified $\sigma(Na^+-O)$ and FQs and **Na4** for both LJ parameters modified and FQs. All σ and ε parameters are reported in Table 3, and the interaction potentials are shown in panel B of Figure 3; the corresponding RDFs and running integrals ($N(r)$) are depicted in panel A of Figure 3. For each potential, a metadynamics simulation was also carried out, and the corresponding results are shown in the following sections. When using metadynamics the r_0 parameter was set to 3.2 Å, with the exception of **Na2** for which a value of 3.3 Å was used.

The **Na1** simulation yields a $g(r)$ with IOD = 2.25 Å and a depletion zone separating the first and second hydration shells located between 2.5 and 3.5 Å; the value of $N(r)$ at the $g(r)$ first minimum (3.1 Å) is 5.6 but the $g(r)$ never approaches zero. In **Na2**, the $g(r)$ shifts to longer distances (IOD = 2.42 Å) and increases its width (a sign of a more disordered first solvation shell); consequently, the separation between the first and second shell decreases further and $N(r)$ at first minimum (3.2 Å) is 5.90. A similar pattern can be observed for the $g(r)$ second peak, which is located at about 4.5 Å with fixed charges and 5.0 Å with fluctuating ones. In order to obtain a first peak position comparable with **Na1**, a σ parameter correction of 0.36 Å was needed (**Na3**), whereas to make the $g(r)$ closer to the fixed charge result (i.e., to obtain a comparable water coordination number and structural disorder) it was necessary to reduce σ by 0.89 Å and also to increase the well depth by 2.4 kJ/mol (**Na4**) (see Figure 3A). From the RDFs obtained with the modified potentials, it can be easily seen that shifting the $g(r)$ maximum to shorter distances also leaded to a somewhat smaller average coordination number as compared to standard GROMOS96 ($N(r)$ = 5.5 at 3.1 Å). On the other hand, the structural disorder of the first shell and the separation between the first and second shell are halfway between the two previous cases:

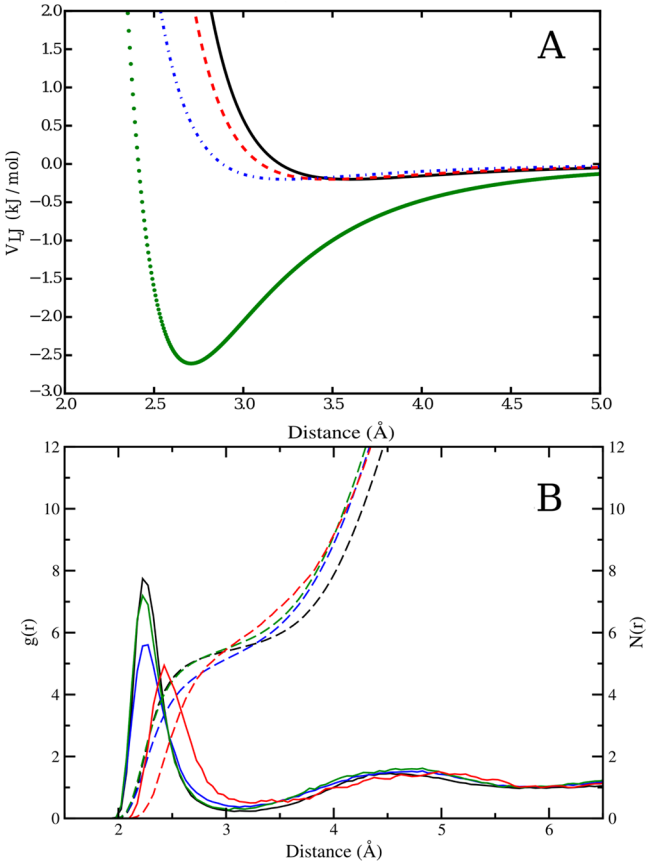

Figure 3. Panel A: Comparison of standard and modified Lennard-Jones potential energies used in Na^+ simulations. The plot shows the results obtained using fixed charges with GROMOS96 parameters (black, **Na1**), fluctuating charges with GROMOS96 parameters (red, **Na2**), fluctuating charges modifying only σ (blue, **Na3**) and fluctuating charges modifying both σ and ε (green, **Na4**). Panel B: comparison of ion−oxygen radial distribution functions (solid lines) and relative integrals (dashed lines) from the Na^+ simulations, using the same color convention as used previously.

when the average Na^+−O distance was shortened also the coordination number was affected but a smaller separation between the first and second shell was also observed with respect to the nonpolarizable simulation. In **Na4**, the corresponding $g(r)$ has comparable width and height with respect to **Na1** and $N(r)$ is 5.8 at about 3.1 Å.

In Table 4, the results obtained in this work are compared to those of three recent studies.[74−76] Concerning IOD values, it can be easily observed that fixed charges; that is, results from **Na1** (and, by construction, **Na3** and **Na4**) yield shorter ion water distances; using polarization without any correction to LJ parameters (simulation **Na2**) shifts the same value to 2.42 Å, within the range of the IOD values issuing from previous

dx.doi.org/10.1021/ct400988e | J. Chem. Theory Comput. 2014, 10, 1150−1163

Table 4. Position of the First Peak of the $g(r)$ (IOD) and the Corresponding Coordination Number at That Distance ($N(r)$) Obtained from Simulations Na1, Na2, Na3, and Na4[a]

	Na1	Na2	Na3	Na4	ref 71	ref 72	ref 73
IOD (Å)	2.25	2.42	2.25	2.25	2.50	2.35−2.38	2.38
$N(r)$	5.6	5.90	5.60	5.90	6.20	NA	6.00

[a]A qualitative comparison is made with data presented in references 74 (Jensen and Jorgensen) 75, (Joung et al.), and 76 (Gladich et al.).

studies (see caption of Table 4). Note that the results shown in Table 4 have been obtained using different computational protocols (including MD or Monte Carlo simulations, different water models, and several ways of treating long-range interactions) and LJ parameters. A comparable improvement is obtained for the hydration number, which is underestimated in **Na1**: with polarization enabled, the ion coordination number is closer to the results obtained in refs 74 and 76. It is worth observing that for Na^+ $N(r)$ values between 4.0 and 8.0[55,56] have been obtained with different computational and experimental methods: this shows that for this ion it is very difficult to obtain a reliable and accurate evaluation of the coordination number.

3.2.2. Free Energy Landscapes and Residence Times. Figure 4 shows the free energy landscapes of ion coordination

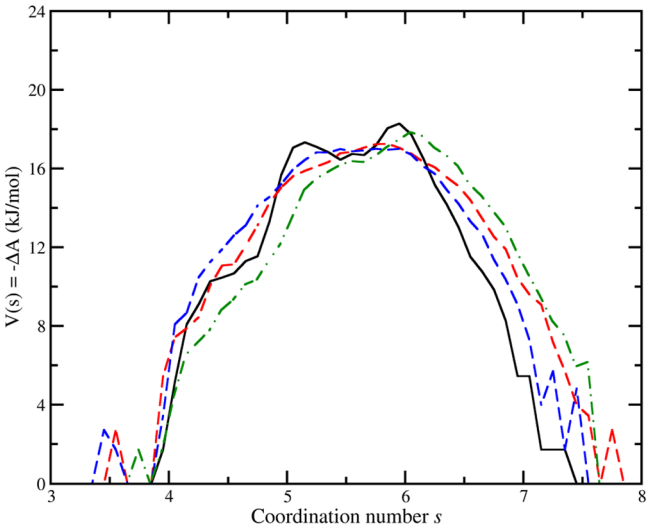

Figure 4. Free energy landscapes of ion coordination issuing from MD simulations of Na^+ in aqueous solution with normal sampling. The plot shows the results obtained using fixed charges with GROMOS96 parameters (black, **Na1**), fluctuating charges with GROMOS96 parameters (red, **Na2**), fluctuating charges modifying only σ (blue, **Na3**) and fluctuating charges modifying both σ and ε (green, **Na4**). Panel B: comparison of standard and modified Lennard-Jones potential energies used in Na^+ simulations, using the same color convention as previously.

evaluated *a posteriori* from standard MD sampling as $-\Delta A = kT \ln P(s)$, where s is the ion coordination number, $P(s)$ is the corresponding probability distribution, k is the Boltzmann constant and T the temperature. The results obtained using metadynamics simulations are shown, for each potential considered (see details above), in Figure 5. In the non-polarizable case, two distinct maxima located at $s = 5.1$ and $s = 6$ and separated by a small but measurable barrier of about 2 kJ/mol do characterize the computed free energy profile; by enabling explicit polarization, in all cases a bell-shaped free energy curve showing roughly one maximum (located between

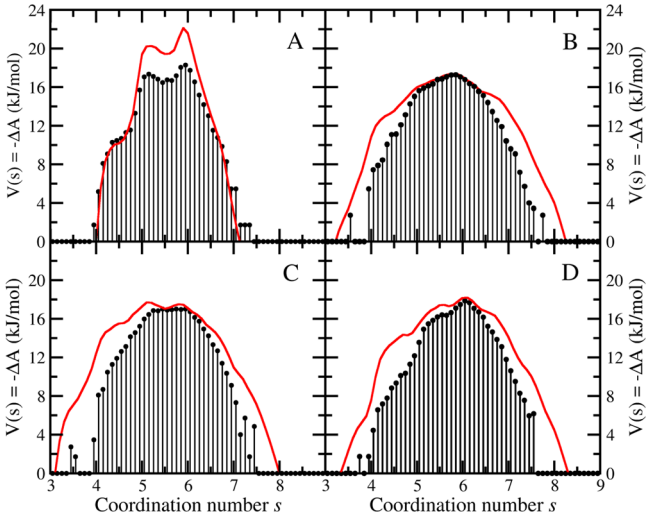

Figure 5. Comparison of free energy profiles of ion coordination obtained using either normal MD sampling (black histograms) or metadynamics simulations (red lines) for Na^+ in water. Top row (panels A and B): trajectories obtained with fixed charges (left, corresponding to **Na1**) and with polarization without any modifications to parameters (right, corresponding to **Na2**). Bottom row (panels C and D): trajectories obtained modifying either only the σ parameter (left, corresponding to **Na3**) or both σ and ε (right, corresponding to **Na4**).

$s = 5.5$, $s = 5.7$, and $s = 6.0$) and possibly some shoulders has been observed. In addition, the nonpolarizable simulation yielded a narrower distribution ($4.0 \le s \le 7.5$) as compared to all trajectories obtained using the FQ model. The smearing and widening of the free energy profiles, as due to the inclusion of explicit polarization, are consistent with the previous analysis of the RDFs. Note that, even when the average IOD and $N(r)$ are very close in both polarizable and nonpolarizable simulations (e.g., in **Na1** and **Na4**), the latter effects are easily noticeable. With metadynamics, in all cases the positions of the stationary points of the ΔA profiles resulted, as expected, in very close agreement with those obtained by standard simulations and both the relative heights and shapes nicely matched. Free energy profiles issuing from the nonpolarizable models are in good agreement with those previously reported,[54] thus showing that the present protocol is still valid when FQ and NPBC are considered. Overall, the same smearing effects observed from standard MD simulations were retained also in metadynamics simulations. For example, by comparing the results obtained with fixed and fluctuating charges modifying only σ, three different preferred coordination numbers, that is, $s = 4$, 5, and 6, have been found. However, while the barrier between the first two peaks was about 10 kJ/mol for fixed charges, it dropped down to 2.5 kJ/mol when using fluctuating charges; similarly, the barrier between $s = 5$ and $s = 6$ dropped from 3 kJ/mol to less than 1 kJ/mol, and the relative stability of the same two hydration structures was switched. In general, when turning on

polarization, the probability to access less favored coordination numbers was remarkably increased, as demonstrated by the wider ΔA profiles along s.

Figure 6 shows the first-shell autocorrelation functions used to calculate the mean residence times (MRT) for all

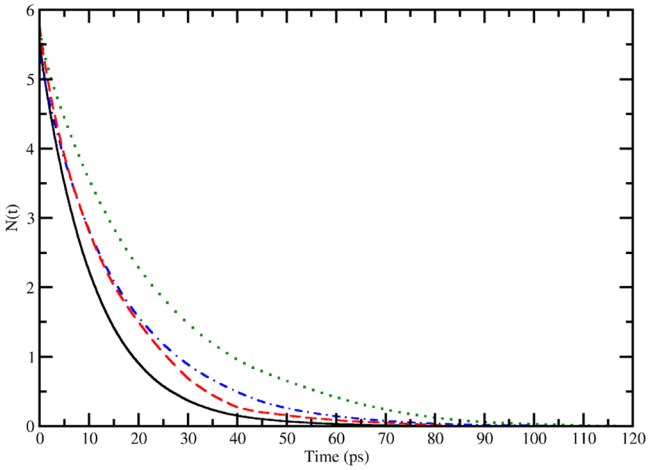

Figure 6. First shell residence time of water molecules obtained from the Na^+ simulations. The plot shows the results obtained using fixed charges with GROMOS96 parameters (black, **Na1**), fluctuating charges with GROMOS96 parameters (dashed red, **Na2**), fluctuating charges modifying only σ (dot-dashed blue, **Na3**), and fluctuating charges modifying both σ and ε (dotted green, **Na4**).

simulations, as obtained by using the Impey method. Based on the $g(r)$, a cutoff radius of 3.1 Å was selected to distinguish between solvent molecules belonging to the first solvation shell and the others, with the exception of **Na2** where a cutoff radius of 3.3 Å was used. The t^* parameter was initially set to 2.0 ps. All curves have shown a monoexponential decay and dropped to zero between 80 ps (nonpolarizable and polarizable simulations with nonmodified LJ potential) and 110 ps (polarizable simulations with modified LJ potentials). MRTs obtained by fitting with an exponential function provided 11.1 ps (**Na1**), 14.5 ps (**Na2**), 16.6 ps (**Na3**), and 22.6 ps (**Na4**). Hence, polarizable MD simulations yielded residence times longer than the nonpolarizable one. This result may appear counterintuitive, even if the observed differences are rather small. The estimation of the mean residence time may be sensitive to the t^* parameter, especially for fast exchanging ions, as pointed out in a recent paper.[77] For this reason, we evaluated the MRTs by changing t^* from 1 to 8 ps in **Na1** and **Na4**: the results varied between 10.82 and 11.78 ps for **Na1** and between 22.06 and 25.4 ps for **Na4**. Thus, even if a small dependence on t^* was obtained, we concluded that the differences in the exchange rates between fixed and fluctuating charge models did not depend on it. On the other hand, since Na^+ is a fast water-exchanging ion and there is no complete separation between hydration shells, kinetic factors depending on water−water interactions may have a significant impact on the exchange rates. To further investigate this point, we estimated the self-diffusion coefficient, D, of water from SPC and SPC-FQ2 simulations. The diffusion constants have been estimated choosing a subset of water molecules initially located within a radius of 5 Å from the center of the sphere and then evaluating their mean square displacements; four short simulations have been performed for each model and only the initial portion of the MSD was used for the fitting, before the initially selected water molecules approached the boundary. The estimated values for D were 4.05×10^{-5} cm^2 s^{-1} and 1.37×10^{-5} cm^2 s^{-1} for nonpolarizable and polarizable water models, respectively. The value for the fixed charge simulation is in acceptable agreement with other results obtained with PBC[78] or NPBC.[41] Therefore, the decreased mobility of water in the polarizable model may well account for the larger residence times observed. It is also worth noting that the experimental value for the self-diffusion coefficient of water is $D \sim 2.3 \times 10^{-5}$ cm^2 s^{-1},[79] significantly smaller than the value obtained by standard SPC and closer to the one obtained with the SPC-FQ2 model. Note that to correctly estimate water exchange rates solute−solvent interactions should be accurately modeled,[80−82] and ion self-diffusion coefficients in the nonpolarizable and polarizable trajectories may also be important; however, in our current protocol, the ions were kept frozen at the center of the box and their mobility was not considered. Besides, in addition to their heights, the widths of the barriers separating the free energy minima (corresponding to stable hydration states) should be also considered: lower but wider barriers may actually slightly increase the residence time by smoothing the configuration transition, particularly if the barrier peak differences are not very large, as in this case.

3.3. Ca^{2+} in Water. An analogous comparison between fixed and fluctuating charges has been carried out for Ca^{2+}. As for Na^+, we adopted the GROMOS96 and the SPC water model. Concerning the polarizable model, test simulations have been performed to optimize the $\sigma(Ca^{2+}-O)$ parameter in order to obtain a position of the $g(r)$ first peak comparable to the results obtained with fixed charges. The final parameters are shown in Table 3, and the resulting Lennard-Jones potential energy is depicted in Figure 7, along with the original one.

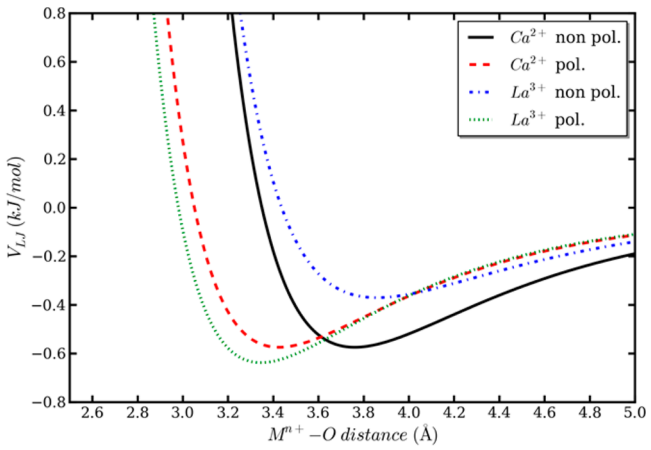

Figure 7. Comparison of standard and modified Lennard-Jones potential energies used in Ca^{2+} and La^{3+} simulations. The full black line represents the standard potential energy taken from GROMOS96 for Ca^{2+}; the red dashed line shows the modified potential used in Ca^{2+} simulations with FQ; the blue dot-dashed line shows the OPLS potential energy for La^{3+} with fixed charges; the green dotted line shows the shifted potential used in La^{3+} simulations with FQ.

Both standard MD and metadynamics simulations have been carried out in order to get a more complete description of the free energy profile of Ca^{2+} coordination in water; the continuous coordination number, s, was defined by setting r_0 = 3.40 Å, according to a previous work by Brancato and Barone.[54] The $g(r)$ and $N(r)$ obtained for Ca^{2+} in water with

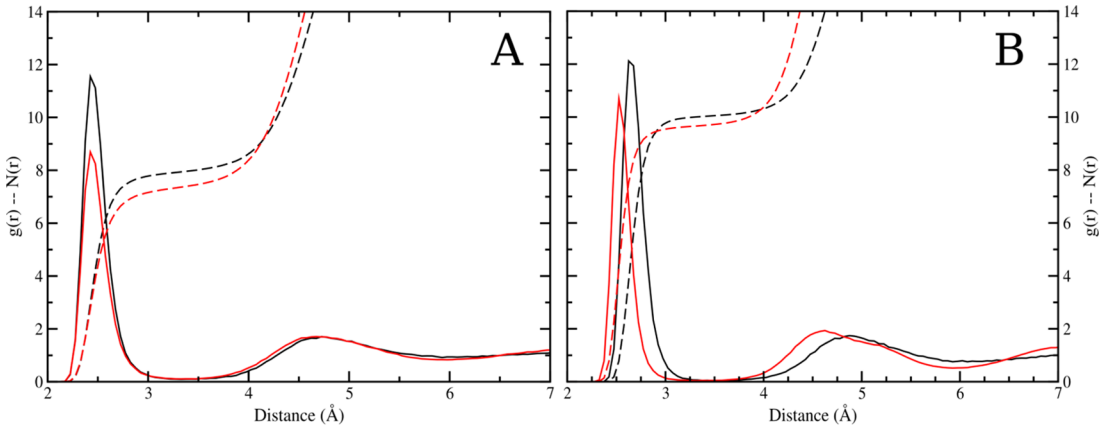

Figure 8. Comparison of ion−oxygen radial distribution functions (full lines) and relative integrals (dashed lines) obtained using either fixed charges (black) or fluctuating ones (red). Panel A: Ca^{2+}−O $g(r)$ and $N(r)$; Panel B: La^{3+}−O $g(r)$ and $N(r)$.

and without explicit polarization are shown in Figure 8 (panel A). Approximately, the same pattern obtained for Na^+ has been observed here: IOD (2.43 Å) is the same in both cases by construction, while polarizable charges caused the height of the $g(r)$ first peak to be reduced, leading to a lower number of water molecules in the first hydration shell. Beyond the first peak, the RDFs are basically superimposable (and again the RDFs did not fall to zero completely). The average hydration number drops from 8 (fixed charges) to 7.5 (polarizable charges) at about 3.4 Å, with the slope of the integral curves being very similar (at variance with Na^+). The two $g(r)$ became indistinguishable at distances longer than 4.5 Å.

Table 5 compares the results obtained in this work to those reported in recent computational studies of Ca^{2+} in aqueous solution.[83,84] As explained, the σ parameter was modified in order to yield, by construction, the same value of IOD obtained in the fixed charge simulation. The results obtained are in good agreement with the data shown in ref 84. Note that the results presented by Todorova et al. were obtained by CPMD trajectories about 7 to 20 ps long and starting with a 6 coordinated Ca^{2+} ion; thus, sampling of $N(r) > 6$ may be affected by poor statistics. In ref 84 the authors showed that, for divalent metal cations, there is no single LJ parameter set able to reproduce at the same time hydration free energies, ion water (first shell) distances and coordination numbers obtained from experimental data and, instead, developed LJ parameters specifically targeting one these properties. In addition to the differences due to variations in the computational protocol (none of the results in refs 83 or 84 were obtained with SPC water or using NPBC), it must also be observed that the survey of recent experimental and computational data included in ref 83 shows IOD variations between 2.39 and 2.46 Å and $N(r)$ values between 5.5 and 10.

Table 5. IOD and $N(r)$ Issuing from Ca^{2+} Simulations Using Either Fixed or Fluctuating Charges[a]

	this work (nonpol.)	this work (pol.)	ref 83	ref 84 (IOD set)
IOD (Å)	2.43	2.43	2.39	2.45−2.47
$N(r)$	8.0	7.5	6.0	7.9−8.0

[a]Data from refs 83 (Todorova et al.) and 84 (Li et al.) are included for comparison.

The ΔA profiles obtained comparing normal sampling and metadynamics are reported in Figure 9 (panels A and B). In both cases, three peaks have been observed, located at s = 7, 8, and 9 (the latter is more properly just a shoulder) but the use of fluctuating charges lowered the relative free energy changes between s = 7 and s = 8 from 10 to 2 kJ/mol and between s = 8 and 9 from 13 to 7 kJ/mol. Also, it is worth noting that the preferred coordination number shifted to lower values when using polarization (the same was observed with Na^+, but the effect is significantly larger here). In addition, the use of fluctuating charges has made accessible to the system also coordination numbers unreachable with fixed charges, as shown by the presence of a fourth peak at s = 6, separated by the most probable value of s = 7 by about 6 kJ/mol. Overall, polarization has reduced the barrier heights between different hydration structures, has made new ones accessible, and has somewhat lowered the average coordination number. This is again fully consistent with the results reported in Figure 7 and qualitatively similar to Na^+, although in this case the same overall effects can be observed more clearly. Finally, the left panel of Figure 9 shows the comparison for the first-shell self-correlation functions obtained with or without polarization, using a cutoff of 3.35 Å and t^* = 2.0 ps; the calculated τ were 50.3 ps (nonpolarizable model) and 70.8 ps (polarizable model). In this case, values of t^* between 1.0 and 8.0 ps yielded residence times between 48.10 and 54.30 ps and between 72.80 and 78.30 ps for the fixed and fluctuating charge simulations, respectively. Again, even if residence times are longer as compared to Na^+, the differences in exchange rates can be mostly ascribed to the diffusion of water according to the two considered models, that is, SPC and SPC-FQ2.

3.4. La^{3+} in Water. The last system considered in this work is a trivalent ion, namely La^{3+} in aqueous solution. In this case, the LJ parameters have been optimized to obtain a favorable comparison with recent experimental results on IOD.[27] The TIP3P (coupled with OPLS[85] parameters) and TIP3P-FQ2 water models have been adopted in this case. In Table 3, we report the LJ parameters used in this work, and in Figure 7, the corresponding modified potential energy. Results issuing from the MD simulations are reported in Figure 8 (panel B) and Figure 9 (panels C and D). The computed $g(r)$ had a comparable first peak widths in the two simulations considered, that is, 0.24 and 0.20 Å for the nonpolarizable and polarizable trajectories, respectively. As noted above, explicit polarization reduced the height of the $g(r)$ and thus the first shell

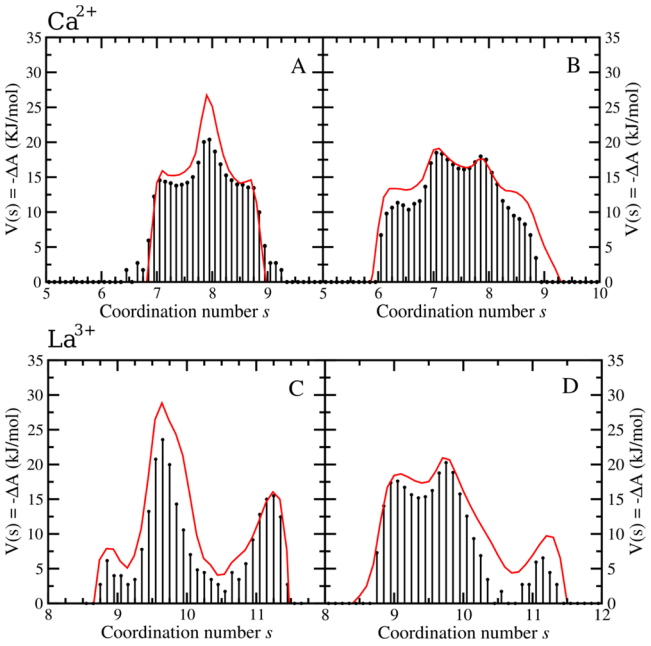

Figure 9. Comparison of free energy profiles for the continuous coordination number, *s*, obtained from standard MD simulations (black histograms) and from metadynamics simulations (red lines) from the Ca^{2+} (top row, panels A and B) and La^{3+} (bottom row, panels C and D) simulations. Graphs on the left side (panels A and C) show results obtained using fixed charges, while those on the right side (panels B and D) contain results yielded by trajectories with fluctuating charges.

coordination number, as calculated from the integral of $g(r)$, is about 10 with fixed charges and 9.5 with fluctuating ones; however, in this case, this phenomenon might also be partially due to shorter average ion−oxygen distance. In both cases, the first and second coordination shell were very well separated with equally wide (0.5 Å) depletion zones, where $g(r) = 0.0$ (at variance with Na^+ and Ca^{2+}); for the fluctuating charge trajectory the depletion zone and second maximum of the $g(r)$ were shifted by 0.12 Å to shorter distances, like the first peak. In this case the use of polarization caused the $g(r)$ second peak to be higher as compared to the nonpolarizable model, and similarly, the second minimum was deeper and the radial distribution function more structured up to a distance of 8.0 Å; this result seems different with respect to the other two cations, where no difference between fixed and fluctuating charges was observed at longer distances.

A comparison of the results obtained in this work with those presented by Duvail et al.[26] and later refined by D'Angelo et al.[27] is shown in Table 6. In this case, the IOD obtained without polarization is longer than values reported in literature (in ref 27, results are in agreement with EXAFS data) and $N(r)$ shows an additional water molecule in the La^{3+} first solvation shell. By modifying the σ parameter in the FQ simulation, we obtain a IOD and N(r) more comparable with the values reported in refs 26 and 27. Concerning the free energy of ion-coordination, both polarizable and nonpolarizable metadynamics simulations have shown three distinct peaks located at about *s* = 9, 10, and 11. In both cases, the most stable peak corresponded to the 10-fold coordination but ΔA between the first two peaks, that is, *s* = 9 and 10, dropped from about 20 to 3 kJ/mol when turning on explicit polarization. On the other hand, the 10-fold and 11-fold configurations were separated in the two cases by a more comparable barrier, about 10 kJ/mol. It can be easily observed that, while the general behavior is qualitatively similar to the results already discussed in terms of decrease of free energy barriers between different maxima, in this case, the effect is much stronger and there are also other remarkable differences. The first-shell exchange relaxation times are reported in Figure 10, panels B and C: the exchange rates were about $\tau = 4200$ ps with fixed charges and 300 ps with fluctuating ones. Such a large discrepancy is consistent with the quite different ΔA barriers observed above, which may overcome other kinetic effects as previously discussed: the estimated *D* for TIP3P and TIP3P-FQ2 water models yielded values of 4.05×10^{-5} cm^2 s^{-1} and 1.58×10^{-5} cm^2 s^{-1}, respectively.

Table 6. IOD and $N(r)$ Issuing from La^{3+} Simulations Using Either Fixed or Fluctuating Charges[a]

	this work (nonpol.)	this work (pol.)	ref 26	ref 27
IOD (Å)	2.65	2.54	2.50−2.58	2.60
$N(r)$	10.0	9.60	9.02	9.10

[a]Data from refs 26 and 27 are included for comparison.

3.5. Comparison of Ion−Water Interaction Energies.

Having discussed at length the perturbations caused by polarization on the structure and dynamics of ions, here we analyze such differences in terms of ion−water interaction energies. We compared the average Coulomb and Lennard-Jones interaction energies between the ion and the water molecules as obtained from the FQ simulations and the energies that would have been obtained using a fixed charge model from the same trajectories. The average energies and energy differences were calculated including an increasing number of water molecules, roughly corresponding to the first, second and third hydration shells, by using a cutoff distance R_C (based on the $g(r)$; see Figures 3B, and 8A and B), and including also a bulk term. To further simplify the comparison, a constant step of 3 Å has been adopted to increase R_C. In the analysis of Na^+, we report only the **Na3** simulation (in which only the value of σ_{Na} was changed). Note, however, that the same calculations performed on simulations **Na2** and **Na4** yielded comparable convergence trends. We also included a bulk water polarization term provided by the continuum Born model, as done by Brancato et al.:[42]

$$E_{cont} = \frac{1}{4\pi\varepsilon_0}\frac{\varepsilon_r - 1}{\varepsilon_r}\frac{q^2}{R_C} \quad (5)$$

where ε_r is the water relative permittivity (a value of 78.0 was used), q is the ion charge, and R_C the cutoff used to include water molecules; note that such a term depends only on the ion charge and on R_C and, thus, is constant along the trajectory, and since the ion charge is fixed, it does not change when using polarization. Table 7 shows the energy differences between fixed and fluctuating charge models (ΔE_{Elec} and ΔE_{LJ}) and also the absolute electrostatic contributions (only for the FQ simulations) including the contribution obtained with eq 5 (E_{Elec} and $E_{Elec+cont}$). First, we observed the convergence of the energy differences for the electrostatic and LJ terms as the cutoff radius increases, where the largest contribution is already provided by the first hydration shell. As in pure water simulations, the trend of the ΔE_{LJ} term is opposed to that of the electrostatic one since, by construction, it was tuned to compensate for the differences induced by switching from fixed

dx.doi.org/10.1021/ct400988e | J. Chem. Theory Comput. 2014, 10, 1150−1163

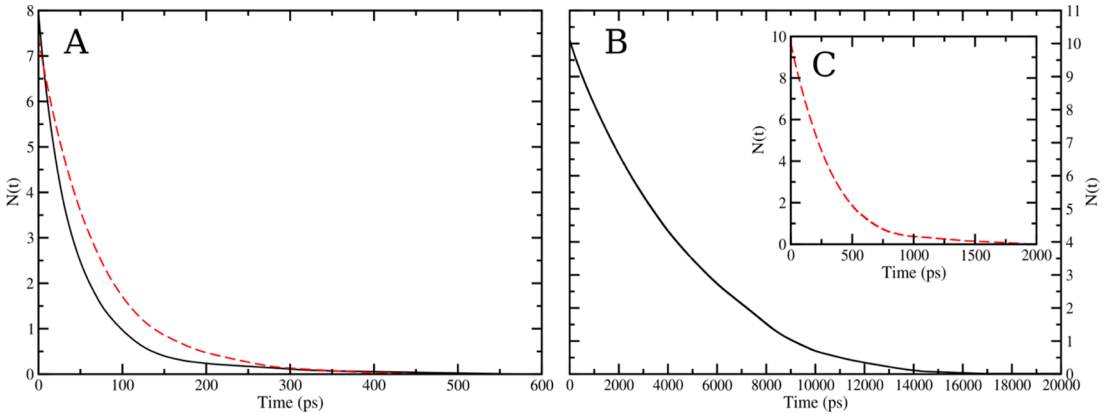

Figure 10. First shell residence times of water molecules from Ca^{2+} (panel A) and La^{3+} (panels B and C) trajectories. The results from simulations with fixed charges are shown using continuous black lines while those obtained using polarization are shown with dashed red lines. Because of their different time scale, the results yielded by La^{3+} simulations are shown in different panels.

Table 7. Potential Energies (Electrostatic and Lennard-Jones) Calculated along the FQ Trajectories and Those That Would Have Been Obtained with a Fixed Charge Topology on the Same Coordinates, Obtained Using Increasing Cut-off Radii (R_C), for the Three Ions, Based on Radial Distribution Functions[a]

ion	R_C (Å)	ΔE_{Elec} (kJ/mol)	ΔE_{LJ} (kJ/mol)	E_{Elec} (kJ/mol)	$E_{Elec+cont}$ (kJ/mol)
Na^+	3.0	−23.49	66.56	−369.60	−655.34
Na^+	6.0	−33.06	65.75	−517.67	−693.51
Na^+	9.0	−37.23	65.58	−584.27	−711.26
Na^+	12.0	−39.33	65.53	−618.47	−717.86
Ca^{2+}	3.5	−68.18	88.25	−1173.05	−2208.17
Ca^{2+}	6.5	−101.78	86.81	−1711.35	−2372.33
Ca^{2+}	9.5	−117.33	86.52	−1957.43	−2442.93
Ca^{2+}	12.5	−125.12	86.45	−2083.35	−2467.00
La^{3+}	3.5	−81.59	408.05	−2345.02	−4674.05
La^{3+}	6.5	−127.28	404.14	−3498.78	−4985.99
La^{3+}	9.5	−150.45	403.23	−4220.78	−5162.71
La^{3+}	12.5	−160.98	403.01	−4329.65	−5192.86

[a]For Na^+, the **Na3** simulation has been used. ΔE_{Elec} and ΔE_{LJ} are the difference obtained applying either the fixed or fluctuating charge topology to the FQ trajectories, while E_{Elec} is the absolute values obtained using FQ parameters for the electrostatic term and $E_{Elec+cont}$ includes the contribution from the continuum estimated as per eq 5.

to fluctuating charges, which are most relevant at short distances. The relative weight of the first shell contribution (and the energy convergence as a function of the R_C value) may also be estimated from the absolute value of the $E_{Elec+cont}$ term, which contains the contribution of the polarizable continuum term given by eq 5. It is also worth observing that water−water energy differences (Table 2) are small as compared to their ion−water counterparts. Moreover, it can be noted that, in analogy with the properties analyzed previously, the differences between fixed and fluctuating charges have a nonlinear trend as a function of the ionic charge.

4. CONCLUSIONS AND PERSPECTIVES

Summarizing, in the present work we carefully analyzed the effects of solvent polarization on the hydration of three aqueous ions of increasing charge. Polarization was described through an effective on-the-fly propagation of Fluctuating Charges coupled with Nonperiodic Boundary Conditions. We would like to point out that the free energy landscapes of ion coordination, as accurately evaluated by an effective computational approach developed in our group, may effectively provide fingerprints of ion microsolvation, thus enriching considerably the information gathered from other basic structural properties, such as the radial distribution functions. In this work, we analyzed the free energy landscapes to unravel in full detail the effects of solvent polarization on ion coordination. Upon enabling atomic polarization, we have observed that the main effect on the free energy profile is a smearing of the energy barriers separating different hydration structures, while making accessible new ones with respect to nonpolarizable models. Such a smearing effect, as caused by the use of FQs, does depend on the ionic charge and appears to have a nonlinear trend: when comparing the differences between fixed and fluctuating charges, the observed effect was greatly enhanced when switching from Ca^{2+} to La^{3+} as compared to Na^+ vs Ca^{2+}. Note that aqueous ions as case studies, present two very important advantages: (1) the absence of other intramolecular dynamical effects to be taken into account (e.g., solute reorientation dynamics) and (2) the absence of any charge transfer between the ion and the solvent (in the current frame of constant molecular charge), so to better focus only on the effects of solvent polarization. Concerning the parametrization work, it is important to observe that comparisons between trajectories obtained with or without explicit polarization are often carried out with specific interaction potentials for either case, with a lack of a complete assessment of the distinct contribution issuing from polarization with respect to other terms. In the specific case of water models, these studies usually directly strive to improve the description of water as compared to standard fixed charge models. The objective of this work was not to find optimal interaction parameters for aqueous ions using the FQ model but rather trying to understand and separate which effects can be *solely* ascribed to solvent polarization, while keeping other conditions as similar as possible. We also reported the ongoing progress of our MD code, which is developed in the framework of the Gaussian suite of programs, and sketched a roadmap that contains ongoing and planned development work. By going beyond the usual "sampling" → "snapshots collection" → "property calculation" procedure, the integrated multiscale protocol that we propose aims at being both physically sound and computationally effective, allowing also to compute either on-

the-fly or *a posteriori* a vast amount of properties, including spectroscopic observables, at the same level of computational accuracy. Some steps in the present development will likely include the use of general virtual sites to allow for the description of out-of-plane polarization in planar molecules and a more general definition of internal coordinates.

AUTHOR INFORMATION

Corresponding Author

*E-mail: giordano.mancini@sns.it.

Notes

The authors declare no competing financial interest.

ACKNOWLEDGMENTS

This work was supported by MIUR through FIRB program contract No. RBFR12ETL5 and RBFR10DAK6, and by ERC Advanced Grant 2012 (No. 320951). The authors thank the DREAMS Lab technical staff for managing the computing facilities at SNS and Dr. Filippo Lipparini for fruitful discussions and help.

REFERENCES

(1) Allen, M. P.; Tildesley, D. J. *Computer Simulation of Liquids*; Clarendon Press; Oxford University Press: Oxford [England]; New York, 1989.

(2) Rapaport, D. C. *The Art of Molecular Dynamics Simulation*, 2nd ed.; Cambridge University Press: Cambridge, U.K.; New York, 2004.

(3) Van Gunsteren, W. F.; Bakowies, D.; Baron, R.; Chandrasekhar, I.; Christen, M.; Daura, X.; Gee, P.; Geerke, D. P.; Glättli, A.; Hünenberger, P. H.; Kastenholz, M. A.; Oostenbrink, C.; Schenk, M.; Trzesniak, D.; van der Vegt, N. F. A.; Yu, H. B. Biomolecular Modeling: Goals, Problems, Perspectives. *Angew. Chem., Int. Ed.* **2006**, *45*, 4064−4092.

(4) Sabin, J. R.; Brändas, E.; Canuto, S. *Advanced Quantum Chemistry*; Academic: London; Burlington, MA, 2010; Vol. *59*.

(5) Barone, V.; Bloino, J.; Monti, S.; Pedone, A.; Prampolini, G. Theoretical Multilevel Approach for Studying the Photophysical Properties of Organic Dyes in Solution. *Phys. Chem. Chem. Phys.* **2010**, *12*, 10550−10561.

(6) Steindal, A. H.; Ruud, K.; Frediani, L.; Aidas, K.; Kongsted, J. Excitation Energies in Solution: The Fully Polarizable QM/MM/PCM Method. *J. Phys. Chem. B* **2011**, *115*, 3027−3037.

(7) Praprotnik, M.; Site, L. D.; Kremer, K. Multiscale Simulation of Soft Matter: From Scale Bridging to Adaptive Resolution. *Annu. Rev. Phys. Chem.* **2008**, *59*, 545−571.

(8) Nagarajan, A.; Junghans, C.; Matysiak, S. Multiscale Simulation of Liquid Water Using a Four-to-One Mapping for Coarse-Graining. *J. Chem. Theory Comput.* **2013**, 131028134645007.

(9) Cieplak, P.; Dupradeau, F.-Y.; Duan, Y.; Wang, J. Polarization Effects in Molecular Mechanical Force Fields. *J. Phys.: Condens. Matter* **2009**, *21*, 333102−333123.

(10) Wang, L.-P.; Chen, J.; Van Voorhis, T. Systematic Parametrization of Polarizable Force Fields from Quantum Chemistry Data. *J. Chem. Theory Comput.* **2013**, *9*, 452−460.

(11) Patel, S.; Brooks, C. L. CHARMM Fluctuating Charge Force Field for Proteins: I. Parameterization and Application to Bulk Organic Liquid Simulations. *J. Comput. Chem.* **2004**, *25*, 1−16.

(12) Patel, S.; Mackerell, A. D.; Brooks, C. L. CHARMM Fluctuating Charge Force Field for Proteins: II Protein/solvent Properties from Molecular Dynamics Simulations Using a Nonadditive Electrostatic Model. *J. Comput. Chem.* **2004**, *25*, 1504−1514.

(13) Cieplak, P.; Caldwell, J.; Kollman, P. Molecular Mechanical Models for Organic and Biological Systems Going beyond the Atom Centered Two Body Additive Approximation: Aqueous Solution Free Energies of Methanol and N-Methyl Acetamide, Nucleic Acid Base, and Amide Hydrogen Bonding and Chloroform/Water Partition Coefficients of the Nucleic Acid Bases. *J. Comput. Chem.* **2001**, *22*, 1048−1057.

(14) Wang, Z.-X.; Zhang, W.; Wu, C.; Lei, H.; Cieplak, P.; Duan, Y. Strike a Balance: Optimization of Backbone Torsion Parameters of AMBER Polarizable Force Field for Simulations of Proteins and Peptides. *J. Comput. Chem.* **2006**, *27*, 781−790.

(15) Ponder, J. W.; Wu, C.; Ren, P.; Pande, V. S.; Chodera, J. D.; Schnieders, M. J.; Haque, I.; Mobley, D. L.; Lambrecht, D. S.; DiStasio, R. A.; Head-Gordon, M.; Clark, G. N. I.; Johnson, M. E.; Head-Gordon, T. Current Status of the AMOEBA Polarizable Force Field. *J. Phys. Chem. B* **2010**, *114*, 2549−2564.

(16) Souaille, M.; Loirat, H.; Borgis, D.; Gaigeot, M. P. MDVRY: A Polarizable Classical Molecular Dynamics Package for Biomolecules. *Comput. Phys. Commun.* **2009**, *180*, 276−301.

(17) Richens, D. T. *The Chemistry of Aqua Ions: Synthesis, Structure, and Reactivity: A Tour through the Periodic Table of the Elements*; J. Wiley: Chichester ; New York, 1997.

(18) Hummer, G.; Pratt, L. R.; García, A. E. Molecular Theories and Simulation of Ions and Polar Molecules in Water. *J. Phys. Chem. A* **1998**, *102*, 7885−7895.

(19) Marcus, Y. Effect of Ions on the Structure of Water: Structure Making and Breaking. *Chem. Rev.* **2009**, *109*, 1346−1370.

(20) Foresman, J. B.; Brooks, C. L. An Ab Initio Study of Hydrated Chloride Ion Complexes: Evidence of Polarization Effects and Nonadditivity. *J. Chem. Phys.* **1987**, *87*, 5892.

(21) Dang, L. X.; Rice, J. E.; Caldwell, J.; Kollman, P. A. Ion Solvation in Polarizable Water: Molecular Dynamics Simulations. *J. Am. Chem. Soc.* **1991**, *113*, 2481−2486.

(22) D'Angelo, P.; Migliorati, V.; Mancini, G.; Barone, V.; Chillemi, G. Integrated Experimental and Theoretical Approach for the Structural Characterization of Hg^{2+} Aqueous Solutions. *J. Chem. Phys.* **2008**, *128*, 084502.

(23) Chillemi, G.; Mancini, G.; Sanna, N.; Barone, V.; Longa, S. D.; Benfatto, M.; Pavel, N. V.; D'Angelo, P. Evidence for Sevenfold Coordination in the First Solvation Shell of Hg(II) Aqua Ion. *J. Am. Chem. Soc.* **2007**, *129*, 5430−5436.

(24) Mancini, G.; Sanna, N.; Barone, V.; Migliorati, V.; D'Angelo, P.; Chillemi, G. Structural and Dynamical Properties of the Hg^{2+} Aqua Ion: A Molecular Dynamics Study. *J. Phys. Chem. B* **2008**, *112*, 4694−4702.

(25) Kowall, T.; Foglia, F.; Helm, L.; Merbach, A. E. Molecular Dynamics Simulation Study of Lanthanide Ions Ln3+ in Aqueous Solution Including Water Polarization. Change in Coordination Number from 9 to 8 along the Series. *J. Am. Chem. Soc.* **1995**, *117*, 3790−3799.

(26) Duvail, M.; Vitorge, P.; Spezia, R. Building a Polarizable Pair Interaction Potential for lanthanoids(III) in Liquid Water: A Molecular Dynamics Study of Structure and Dynamics of the Whole Series. *J. Chem. Phys.* **2009**, *130*, 104501.

(27) D'Angelo, P.; Zitolo, A.; Migliorati, V.; Chillemi, G.; Duvail, M.; Vitorge, P.; Abadie, S.; Spezia, R. Revised Ionic Radii of Lanthanoid-(III) Ions in Aqueous Solution. *Inorg. Chem.* **2011**, *50*, 4572−4579.

(28) Villa, A.; Hess, B.; Saint-Martin, H. Dynamics and Structure of Ln(III)−Aqua Ions: A Comparative Molecular Dynamics Study Using Ab Initio Based Flexible and Polarizable Model Potentials. *J. Phys. Chem. B* **2009**, *113*, 7270−7281.

(29) Pratt, L. R.; LaViolette, R. A.; Gomez, M. A.; Gentile, M. E. Quasi-Chemical Theory for the Statistical Thermodynamics of the Hard-Sphere Fluid †. *J. Phys. Chem. B* **2001**, *105*, 11662−11668.

(30) Lipparini, F.; Barone, V. Polarizable Force Fields and Polarizable Continuum Model: A Fluctuating Charges/PCM Approach. 1. Theory and Implementation. *J. Chem. Theory Comput.* **2011**, *7*, 3711−3724.

(31) Rick, S. W.; Stuart, S. J.; Berne, B. J. Dynamical Fluctuating Charge Force Fields: Application to Liquid Water. *J. Chem. Phys.* **1994**, *101*, 6141−6156.

(32) Rick, S. W.; Stuart, S. J.; Bader, J. S.; Berne, B. J. Fluctuating Charge Force Fields for Aqueous Solutions. *Stud. Phys. Theor. Chem.* **1995**, *83*, 31−40.

(33) Rick, S. W.; Berne, B. J. Dynamical Fluctuating Charge Force Fields: The Aqueous Solvation of Amides. *J. Am. Chem. Soc.* **1996**, *118*, 672−679.
(34) Elstner, M.; Porezag, D.; Jungnickel, G.; Elsner, J.; Haugk, M.; Frauenheim, T.; Suhai, S.; Seifert, G. Self-Consistent-Charge Density-Functional Tight-Binding Method for Simulations of Complex Materials Properties. *Phys. Rev. B* **1998**, *58*, 7260−7268.
(35) Trani, F.; Barone, V. Silicon Nanocrystal Functionalization: Analytic Fitting of DFTB Parameters. *J. Chem. Theory Comput.* **2011**, *7*, 713−719.
(36) Van Duin, A. C. T.; Dasgupta, S.; Lorant, F.; Goddard, W. A. ReaxFF: A Reactive Force Field for Hydrocarbons. *J. Phys. Chem. A* **2001**, *105*, 9396−9409.
(37) Smith, P. E.; Pettitt, B. M. Peptides in Ionic Solutions: A Comparison of the Ewald and Switching Function Techniques. *J. Chem. Phys.* **1991**, *95*, 8430−8441.
(38) Martyna, G. J.; Tuckerman, M. E. A Reciprocal Space Based Method for Treating Long Range Interactions in Ab Initio and Force-Field-Based Calculations in Clusters. *J. Chem. Phys.* **1999**, *110*, 2810−2821.
(39) Kastenholz, M. A.; Hünenberger, P. H. Influence of Artificial Periodicity and Ionic Strength in Molecular Dynamics Simulations of Charged Biomolecules Employing Lattice-Sum Methods. *J. Phys. Chem. B* **2004**, *108*, 774−788.
(40) Kastenholz, M. A.; Hünenberger, P. H. Computation of Methodology-Independent Ionic Solvation Free Energies from Molecular Simulations. I. The Electrostatic Potential in Molecular Liquids. *J. Chem. Phys.* **2006**, *124*, 124106.
(41) Brancato, G.; Di Nola, A.; Barone, V.; Amadei, A. A Mean Field Approach for Molecular Simulations of Fluid Systems. *J. Chem. Phys.* **2005**, *122*, 154109.
(42) Brancato, G.; Rega, N.; Barone, V. Reliable Molecular Simulations of Solute−Solvent Systems with a Minimum Number of Solvent Shells. *J. Chem. Phys.* **2006**, *124*, 214505.
(43) Brancato, G.; Barone, V.; Rega, N. Theoretical Modeling of Spectroscopic Properties of Molecules in Solution: Toward an Effective Dynamical Discrete/Continuum Approach. *Theor. Chem. Acc.* **2007**, *117*, 1001−1015.
(44) Brancato, G.; Rega, N.; Barone, V. A Hybrid Explicit/implicit Solvation Method for First-Principle Molecular Dynamics Simulations. *J. Chem. Phys.* **2008**, *128*, 144501.
(45) Tomasi, J.; Mennucci, B.; Cammi, R. Quantum Mechanical Continuum Solvation Models. *Chem. Rev.* **2005**, *105*, 2999−3094.
(46) Frisch, M. J.; Trucks, G. W.; Schlegel, H. B.; Scuseria, G. E.; Robb, M. A.; Cheeseman, J. R.; Scalmani, G.; Barone, V.; Mennucci, B.; Petersson, G. A.; Nakatsuji, H.; Caricato, M.; Li, X.; Hratchian, H. P.; Izmaylov, A. F.; Bloino, J.; Zheng, G.; Sonnenberg, J. L.; Hada, M.; Ehara, M.; Toyota, K.; Fukuda, R.; Hasegawa, J.; Ishida, M.; Nakajima, T.; Honda, Y.; Kitao, O.; Nakai, H.; Vreven, T.; Montgomery, J. A., Jr.; Peralta, J. E.; Ogliaro, F.; Bearpark, M.; Heyd, J. J.; Brothers, E.; Kudin, K. N.; Staroverov, V. N.; Kobayashi, R.; Normand, J.; Raghavachari, K.; Rendell, A.; Burant, J. C.; Iyengar, S. S.; Tomasi, J.; Cossi, M.; Rega, N.; Millam, N. J.; Klene, M.; Knox, J. E.; Cross, J. B.; Bakken, V.; Adamo, C.; Jaramillo, J.; Gomperts, R.; Stratmann, R. E.; Yazyev, O.; Austin, A. J.; Cammi, R.; Pomelli, C.; Ochterski, J. W.; Martin, R. L.; Morokuma, K.; Zakrzewski, V. G.; Voth, G. A.; Salvador, P.; Dannenberg, J. J.; Dapprich, S.; Daniels, A. D.; Farkas, Ö.; Foresman, J. B.; Ortiz, J. V.; Cioslowski, J.; Fox, D. J. *Gaussian 09*, Revision D.01; Gaussian, Inc.: Wallingford, CT, 2009.
(47) Lipparini, F.; Scalmani, G.; Mennucci, B.; Frisch, M. J. Self-Consistent Field and Polarizable Continuum Model: A New Strategy of Solution for the Coupled Equations. *J. Chem. Theory Comput.* **2011**, *7*, 610−617.
(48) Lipparini, F.; Stamm, B.; Cancès, E.; Maday, Y.; Mennucci, B. Fast Domain Decomposition Algorithm for Continuum Solvation Models: Energy and First Derivatives. *J. Chem. Theory Comput.* **2013**, *9*, 3637−3648.
(49) Sherwood, P.; de Vries, A. H.; Guest, M. F.; Schreckenbach, G.; Catlow, C. R. A.; French, S. A.; Sokol, A. A.; Bromley, S. T.; Thiel, W.; Turner, A. J.; Billeter, S.; Terstegen, F.; Thiel, S.; Kendrick, J.; Rogers, S. C.; Casci, J.; Watson, M.; King, F.; Karlsen, E.; Sjøvoll, M.; Fahmi, A.; Schäfer, A.; Lennartz, C. QUASI: A General Purpose Implementation of the QM/MM Approach and Its Application to Problems in Catalysis. *J. Mol. Struct. THEOCHEM* **2003**, *632*, 1−28.
(50) Miyamoto, S.; Kollman, P. A. Settle: An Analytical Version of the SHAKE and RATTLE Algorithm for Rigid Water Models. *J. Comput. Chem.* **1992**, *13*, 952−962.
(51) Berendsen, H. J. C.; Postma, J. P. M.; van Gunsteren, W. F.; DiNola, A.; Haak, J. R. Molecular Dynamics with Coupling to an External Bath. *J. Chem. Phys.* **1984**, *81*, 3684.
(52) Bussi, G.; Donadio, D.; Parrinello, M. Canonical Sampling through Velocity Rescaling. *J. Chem. Phys.* **2007**, *126*, 014101.
(53) Laio, A.; Parrinello, M. Escaping Free-Energy Minima. *Proc. Natl. Acad. Sci.* **2002**, *99*, 12562−12566.
(54) Brancato, G.; Barone, V. Free Energy Landscapes of Ion Coordination in Aqueous Solution. *J. Phys. Chem. B* **2011**, *115*, 12875−12878.
(55) Marcus, Y. Ionic Radii in Aqueous Solutions. *Chem. Rev.* **1988**, *88*, 1475−1498.
(56) Ohtaki, H.; Radnai, T. Structure and Dynamics of Hydrated Ions. *Chem. Rev.* **1993**, *93*, 1157−1204.
(57) Helm, L.; Merbach, A. E. Inorganic and Bioinorganic Solvent Exchange Mechanisms. *Chem. Rev.* **2005**, *105*, 1923−1960.
(58) D'Angelo, P.; Spezia, R. Hydration of Lanthanoids(III) and Actinoids(III): An Experimental/Theoretical Saga. *Chem.—Eur. J.* **2012**, *18*, 11162−11178.
(59) Jorgensen, W. L. Quantum and Statistical Mechanical Studies of Liquids. 10. Transferable Intermolecular Potential Functions for Water, Alcohols, and Ethers. Application to Liquid Water. *J. Am. Chem. Soc.* **1981**, *103*, 335−340.
(60) Berendsen, H. J. C.; Postma, J. P. M.; Van Gunsteren, W. F.; Hermans, J. Interaction Models for Water in Relation to Protein Hydration. *Intermolecular Forces* **1981**, *11*, 331−342.
(61) Mortier, W. J.; Van Genechten, K.; Gasteiger, J. Electronegativity Equalization: Application and Parametrization. *J. Am. Chem. Soc.* **1985**, *107*, 829−835.
(62) Rappe, A. K.; Goddard, W. A., III Charge Equilibration for Molecular Dynamics Simulations. *J. Phys. Chem.* **1991**, *95*, 3358−3363.
(63) Torrie, G. M.; Valleau, J. P. Nonphysical Sampling Distributions in Monte Carlo Free-Energy Estimation: Umbrella Sampling. *J. Comput. Phys.* **1977**, *23*, 187−199.
(64) Torda, A. E.; van Gunsteren, W. F. Algorithms for Clustering Molecular Dynamics Configurations. *J. Comput. Chem.* **1994**, *15*, 1331−1340.
(65) Grubmüller, H. Predicting Slow Structural Transitions in Macromolecular Systems: Conformational Flooding. *Phys. Rev. E* **1995**, *52*, 2893−2906.
(66) Kumar, S.; Rosenberg, J. M.; Bouzida, D.; Swendsen, R. H.; Kollman, P. A. The Weighted Histogram Analysis Method for Free-Energy Calculations on Biomolecules. I. The Method. *J. Comput. Chem.* **1992**, *13*, 1011−1021.
(67) Maragliano, L.; Vanden-Eijnden, E. A Temperature Accelerated Method for Sampling Free Energy and Determining Reaction Pathways in Rare Events Simulations. *Chem. Phys. Lett.* **2006**, *426*, 168−175.
(68) Andersen, H. C. Molecular Dynamics Simulations at Constant Pressure and/or Temperature. *J. Chem. Phys.* **1980**, *72*, 2384.
(69) Impey, R. W.; Madden, P. A.; McDonald, I. R. Hydration and Mobility of Ions in Solution. *J. Phys. Chem.* **1983**, *87*, 5071−5083.
(70) Soper, A. K. The Radial Distribution Functions of Water as Derived from Radiation Total Scattering Experiments: Is There Anything We Can Say for Sure? *ISRN Phys. Chem.* **2013**, *2013*, 1−67.
(71) Mahoney, M. W.; Jorgensen, W. L. A Five-Site Model for Liquid Water and the Reproduction of the Density Anomaly by Rigid, Nonpolarizable Potential Functions. *J. Chem. Phys.* **2000**, *112*, 8910−8922.

(72) Panagiotopoulos, A. Z.; Kiyohara, K.; Gubbins, K. E. Phase Coexistence Properties of Polarizable Water Models. *Mol. Phys.* **1998**, *94*, 803−808.
(73) Gunsteren, W. F. van *Biomolecular Simulation: The GROMOS96 Manual and User Guide*; Biomos: Zürich, Hochschulverlag AG an der ETH Zürich: Zürich; Groningen, 1996.
(74) Jensen, K. P.; Jorgensen, W. L. Halide, Ammonium, and Alkali Metal Ion Parameters for Modeling Aqueous Solutions. *J. Chem. Theory Comput.* **2006**, *2*, 1499−1509.
(75) Joung, I. S.; Cheatham, T. E. Determination of Alkali and Halide Monovalent Ion Parameters for Use in Explicitly Solvated Biomolecular Simulations. *J. Phys. Chem. B* **2008**, *112*, 9020−9041.
(76) Gladich, I.; Shepson, P.; Szleifer, I.; Carignano, M. Halide and Sodium Ion Parameters for Modeling Aqueous Solutions in TIP5P-Ew Water. *Chem. Phys. Lett.* **2010**, *489*, 113−117.
(77) Laage, D.; Hynes, J. T. On the Residence Time for Water in a Solute Hydration Shell: Application to Aqueous Halide Solutions. *J. Phys. Chem. B* **2008**, *112*, 7697−7701.
(78) Wu, Y.; Tepper, H. L.; Voth, G. A. Flexible Simple Point-Charge Water Model with Improved Liquid-State Properties. *J. Chem. Phys.* **2006**, *124*, 024503.
(79) Mahoney, M. W.; Jorgensen, W. L. Diffusion Constant of the TIP5P Model of Liquid Water. *J. Chem. Phys.* **2001**, *114*, 363−366.
(80) Brookes, R.; Davies, A.; Ketwaroo, G.; Madden, P. A. Diffusion Coefficients in Ionic Liquids: Relationship to the Viscosity †. *J. Phys. Chem. B* **2005**, *109*, 6485−6490.
(81) Salanne, M.; Simon, C.; Turq, P.; Madden, P. A. Conductivity−Viscosity−Structure: Unpicking the Relationship in an Ionic Liquid †. *J. Phys. Chem. B* **2007**, *111*, 4678−4684.
(82) Martelli, F.; Vuilleumier, R.; Simonin, J.-P.; Spezia, R. Varying the Charge of Small Cations in Liquid Water: Structural, Transport, and Thermodynamical Properties. *J. Chem. Phys.* **2012**, *137*, 164501.
(83) Todorova, T.; Hünenberger, P. H.; Hutter, J. Car−Parrinello Molecular Dynamics Simulations of $CaCl_2$ Aqueous Solutions. *J. Chem. Theory Comput.* **2008**, *4*, 779−789.
(84) Li, P.; Roberts, B. P.; Chakravorty, D. K.; Merz, K. M. Rational Design of Particle Mesh Ewald Compatible Lennard-Jones Parameters for +2 Metal Cations in Explicit Solvent. *J. Chem. Theory Comput.* **2013**, *9*, 2733−2748.
(85) Jorgensen, W. L.; Maxwell, D. S.; Tirado-Rives, J. Development and Testing of the OPLS All-Atom Force Field on Conformational Energetics and Properties of Organic Liquids. *J. Am. Chem. Soc.* **1996**, *118*, 11225−11236.